International Journal of Bioprinting

RESEARCH ARTICLE

Melt electrowriting-printed peritoneal scaffold prevents peritoneal adhesion and facilitates peritoneal repair

Sicheng Li[1†], Jinjian Huang[1†], Ziyan Xu[2†], Ye Liu[3], Huajian Ren[1], Ze Li[1], Canwen Chen[1], Kang Chen[1], Xiuwen Wu[1*], Jianan Ren[1*]

[1]Research Institute of General Surgery, Affiliated Jinling Hospital, Medical School of Nanjing University, Nanjing 210002, P. R. China

[2]Department of General Surgery, Nanjing First Hospital, Nanjing 210000, P. R. China

[3]Research Institute of General Surgery, Jinling Hospital, School of Medicine, Southeast University, Nanjing 210009, P. R. China

(This article belongs to the *Special Issue: 3D Printing in tissue engineering*)

Abstract

Peritoneal adhesion is a critical issue after abdominal surgery. Cell-based methods for preventing peritoneal adhesion have not yet been fully investigated. Here, we constructed a highly biomimetic peritoneal scaffold by seeding mesothelial cells, the natural physiological barrier of the peritoneum, onto a melt electrowriting-printed scaffold. The scaffolds with the microfibers crossed at different angles (30°, 60°, and 90°) were screened based on mesothelial cell proliferation and orientation. Thirty degrees were more suitable for improving proliferation of mesothelial cells and cell growth in a single direction; therefore, the 30° peritoneal scaffold could better mimic the physiological structure of native peritoneum. Mechanistically, such a peritoneal scaffold was able to act as a barrier to prevent peritoneal resident macrophages from migrating to the site of the peritoneal lesion. *In vivo* mesothelial cell tracking using lentivirus technology confirmed that the peritoneal scaffold, compared to the scaffold without mesothelial cells, could prevent peritoneal adhesion and was directly involved in the repair of injured peritoneum. This study suggests that the peritoneal scaffolds can potentially prevent peritoneal adhesion, offering a new approach for clinical treatment.

Keywords: Melt electrowriting; Peritoneal adhesions; Peritoneal mesothelial cells

†These authors contributed equally to this work.

***Corresponding authors:**
Xiuwen Wu
(wuxiuwen@nju.edu.cn)

Jianan Ren
(jiananr@nju.edu.cn)

Citation: Li S, Huang J, Xu Z, *et al*., 2023, Melt electrowriting-printed peritoneal scaffold prevents peritoneal adhesion and facilitates peritoneal repair. *Int J Bioprint,* 9(3): 682.
https://doi.org/10.18063/ijb.682

Received: November 13, 2022
Accepted: December 02, 2022
Published Online: February 10, 2023

1. Introduction

Peritoneal adhesion is the most common postoperative complication, which can lead to adhesive bowel obstruction, chronic abdominal pain, and infertility[1,2]. The occurrence of postoperative peritoneal adhesions and their complications places a huge burden on patients[3]. In 2020, a study published in the *Lancet* showed that during a 5-year follow-up period, 26.7% of patients had an average of 1.7 readmissions for adhesion-related complications[4]. Adhesive bowel obstruction is the most frequent manifestation of peritoneal adhesion[3], which results in direct hospitalization costs of up to $3.45 billion annually in the USA[5].

The most popular method to prevent postoperative peritoneal adhesion is the implantation of biomaterial products, including artificial films, fluids, or gels[6]. These methods, however, do not completely resolve the problem of peritoneal adhesion[7,8]. There are two important approaches to prevent peritoneal adhesions: (i) blocking the contact of injured visceral organs with neighboring tissues, and (ii) repairing damaged peritoneum. Peritoneal injury forms unintended tissue connections, upon which progressive fibrosis and vascularization enhance the connections. Therefore, the design of biomaterials that can interrupt the connections is a research hotspot.

In recent years, cell therapy has become the frontier of preventing peritoneal adhesion, but there are still some limitations[9]. For example, Tomoya *et al.* prevented peritoneal adhesions by inducing *in situ* barrier formation of abdominal macrophages through injection of interleukin-4c[10]. The effect of drug-induced cell barriers is uncertain because of the heterogeneous immune response capacity of the body. Inagaki *et al.* fabricated cell sheets from fetal liver mesothelial cells, which prevented postoperative adhesions and promoted liver regeneration[11]. However, simple mesothelial cell sheets are mechanically weak and hard to fix surgically, making it difficult to meet real clinical scenario requirements.

In this study, we designed a novel peritoneal scaffold based on the constitution and function of native peritoneum. The human peritoneum is a complex tissue mainly composed of mesothelial cells[12], which forms a natural physiological barrier against organ adhesion and abrasion[13]. Peritoneum is capable of regeneration via a unique healing mechanism through which mesothelial cells migrate from the lesion edge to the center, and detach and settle on the lesion site from opposite or distant areas. These free-floating mesothelial cells, detected in the plasma fluid, proliferate and disperse to repopulate the injured area[14,15]. This method of peritoneal repair enables us to construct a mesothelial cell barrier that blocks peritoneal adhesion to organs and participates in repairing the damaged peritoneum[16].

To provide a carrier for the growth of mesothelial cells, we applied three-dimensional (3D) printing technology to fabricate a scaffold suitable for cell growth[17]. This will provide a stable growth environment for mesothelial cell attachment with appropriate mechanical strength. 3D printing technology has the natural advantage of customization[18,19]. The low technical precision (100–200 μm) of conventional 3D printing, such as fused deposition modeling, and the uncontrollable morphology of electrostatic spun jet fibers fail to provide a suitable scaffold for mesothelial cells. The newly developed melt electrowriting (MEW) technology can overcome the above-mentioned drawbacks[20]. MEW enables highly controllable deposition of ultrafine fibers, which can provide a mechanical support for cell implantation and facilitate the guidance of cell orientation due to its ordered structure[21].

We designed a peritoneal scaffold by seeding primary peritoneal mesothelial cells onto an MEW-printed polycaprolactone (PCL) scaffold, thereby mimicking the native peritoneum (Scheme 1). The scaffold prevented the formation of peritoneal adhesions with synergistic effects by providing a physical and biological barrier against macrophage infiltration, and participated in peritoneal repair.

2. Materials and methods

2.1. Fabrication of PCL scaffolds with MEW

The scaffolds with the fibers in different crossing angles (30°, 60°, and 90°) were fabricated based on a custom-built MEW printing device (EFL-MDW5800; Suzhou Intelligent Manufacturing Research Institute, China). The device consists of motorized XYZ stages with a collector, syringe with a nozzle, two heaters for heating the PCL polymer (CAPA6800; Perstorp Co., Ltd, Sweden), high-voltage generator, and pneumatic system to adjust the extrusion pressure. During printing, the syringe and nozzle was heated to 85°C, and melted PCL was extruded through a syringe with a 150-μm nozzle. The pumped air pressure was 120 kPa, the distance between collector and nozzle was 2.5 mm, the voltage was set at 4500 V, and the printing speed was 80 cm/min.

2.2. Observation of the microstructure

The structure images of PCL scaffolds with the fibers crossed in varied angles (30°, 60°, and 90°) were recorded with a scanning electron microscope (TM3000; Hitachi, Japan). The scaffolds with varied crossing angles were imaged after being coated with a thin layer of gold.

2.3. Measurements of mechanical strength

The stretching capabilities of PCL scaffolds with the fibers in different crossing angles (30°, 60°, and 90°) were tested by a universal material testing machine (CMT2103; MTS, Eden Prairie, MN, USA) according to the regular method used in our laboratory[22]. The PCL scaffolds were tailored with a length of 20 mm, width of 10 mm, and thickness of 10-layer PCL sheets. After the PCL scaffolds were clamped by two parallel metal clips, the upper clip stretched the PCL scaffolds at a rate of 10 mm/min until the scaffolds were torn up. In this way, the tensile stress (τ)–strain (ε) curve could be drawn. The fracture energy (U) of the PCL scaffolds was calculated using Equation I by figuring out

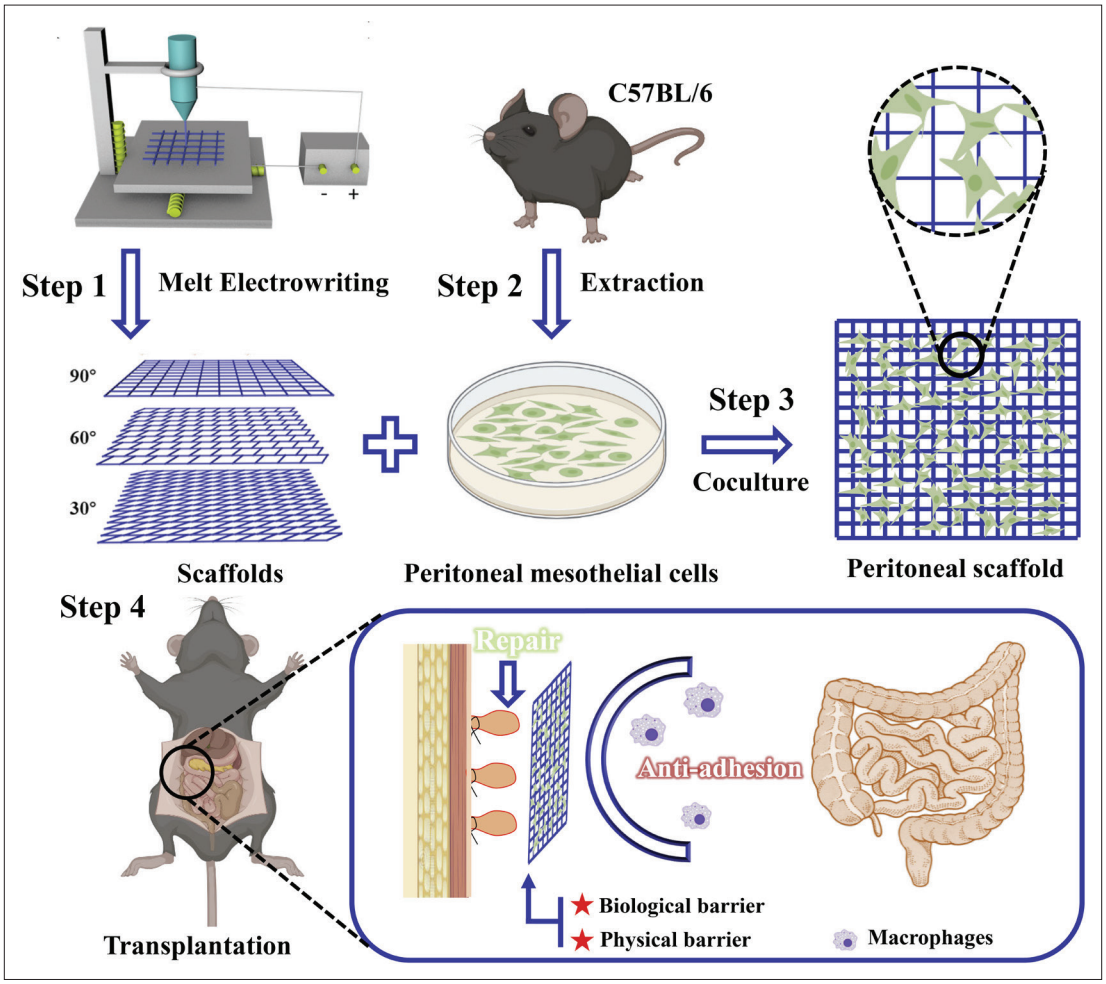

Scheme 1. Fabrication and mechanism of peritoneal scaffolds in the prevention of peritoneal adhesions. Step 1: scaffolds with different pore shapes were constructed using MEW technology. Step 2: Peritoneal mesothelial cells were extracted from mice for *in vitro* expansion and culture. Step 3: Peritoneal mesothelial cells were cocultured with the scaffold. Step 4: Scaffolds loaded with peritoneal mesothelial cells were transplanted to prevent peritoneal adhesion.

the integral of the area under the tensile stress (τ)–strain (ε) curve.

$$U = \int \tau d\varepsilon \quad (I)$$

2.4. Detection of contact angles

The contact angles of PCL scaffolds were determined at room temperature using a contact angle goniometer (SZ-CAMD33; Shanghai Sunzern Instrument Co. Ltd., China) by the sessile drop method. The value of each sample was measured in triplicate.

2.5. Isolation and culture of primary mesothelial cells

After killing the mice, they were soaked in 75% alcohol for 5 min, moved to an ultraclean bench, and placed in supine position during the experiment. The skin was then cut along the midline of the abdomen, and the peritoneal tissue was removed aseptically and immersed in phosphate-buffered saline (PBS) containing penicillin-streptomycin antibiotics, and cut into 1-mm pieces. The tissues were washed twice with PBS and digested with trypsin (PB180225; Procell Life Science and Technology Co. Ltd., Wuhan, China) for 20 min in a water bath at 37°C. The trypsin reaction was terminated by adding complete culture medium of mouse peritoneal mesothelial cells. The cell suspension was gently resuspended by pipette until there was no lumpy tissue, and then centrifuged at 200 × *g* for 8 min after passing through a 100-μm mesh sieve. Cell precipitate was retained, while supernatant was discarded. The cells were resuspended with complete medium of mouse peritoneal mesothelial cell and inoculated in a culture dish precoated with polylysine at 37°C in a 5% CO_2 incubator.

2.6. Degradation experiment *in vivo*

The peritoneal scaffolds measuring 0.5 × 0.5 cm were fixed onto the peritoneum of mice. At each predesignated

interval, three mice were killed, and the peritoneal tissues were harvested at the scaffold suture site for hematoxylin–eosin (HE) staining.

2.7. Preparation and identification of peritoneal scaffolds

Primary peritoneal mesothelial cells were seeded onto the scaffolds and inoculated with the mesothelial cell culture medium (CM-M170; Procell Life Science and Technology Co. Ltd.) in 24-well low-adhesion plates (3473; Corning, Corning, NY, USA). Freshly isolated primary mesothelial cells (0.75×10^6) were suspended in 50 μL of each sample in tissue culture-treated 24-well plates. To promote cell adhesion, cells were incubated at 37°C with 5% CO_2 for 0.5 h, followed by adding 1 mL of cell culture medium.

2.8. Isolation of peritoneal resident macrophages

After the mice were killed, they were soaked in 75% alcohol for 10 s. The mice were removed from alcohol, drained, and placed in the supine position on the ultraclean bench. The abdominal cavity was gently rubbed for 2 min to allow the physiological saline to flow in the cavity after 6 mL of saline was added into the cavity with a syringe. The lower abdominal skin was lifted with ophthalmic forceps so that the animal tilted to one side. After cutting the abdominal skin, a small incision was made in the muscle layer, and the abdominal fluid was aspirated with a rubber-tipped dropper and transferred into a centrifuge tube. The aspiration volume was 4–5 mL per mouse. The collected peritoneal lavage fluid was centrifuged at 1000 r/min for 10 min at 4°C. The supernatant was removed, and 10% high-sugar Dulbecco's modified Eagle's medium (DMEM) was added before cell counting using a cell counting plate. Macrophages were counted under a microscope. The cell concentration was adjusted to the desired level. Cells were inoculated into culture flasks and incubated at 37°C for 4 h. After full wall attachment, the supernatant was discarded, and the nonadherent cells were removed. Afterward, high-sugar DMEM was added, and the culture flasks were returned to the incubator.

2.9. Cell migration assay

Migration assays of the peritoneal resident macrophages were performed using an 8-μm pore size polyester membrane Transwell (Corning). The scaffolds were trimmed to completely cover the bottom layer of the upper chamber of the Transwell. The control group was not covered with any object; the blank group was covered with a scaffold that did not carry cells; and the experimental group was covered with a peritoneal scaffold that carried mesothelial cells. Five hundred microliters of 20% fetal bovine serum-DMEM was dispensed per well in the lower chamber of the Transwell. Cell-tracker Green (C2925; Thermo Scientific, USA) -labeled, serum-free DMEM-solubilized peritoneal resident macrophages (6×10^4) were inoculated into the upper chamber of the Transwell at 100 μL per well. Peritoneal resident macrophages were allowed to migrate across the Transwell membrane for 12 h. The remaining cells in the upper chamber were scraped out with a cotton swab, and the migrating macrophages at the bottom of the upper chamber were detected by immunofluorescence.

2.10. Fluorescent staining

To detect the morphology of peritoneal mesothelial cells seeded on the scaffolds, the staining of CK-18 (ab24561; Abcam, Cambridge, MA, USA) and 4′,6-diamidino-2-phenylindole (DAPI; ab104139; Abcam) was performed as described previously[23]. The slides with cells on them were then washed three times in PBS, fixed for 15 min in 4% paraformaldehyde, permeabilized for 15 min in 0.5% Triton X-100, and blocked for 30 min in 1% bovine serum albumin. Samples were incubated in CK-18 solution at 1:200 for 45 min, and DAPI solution at 1:1000 for 6 min, both in the dark at 37°C. Samples were imaged using confocal laser scanning microscopy. Cross-sectional photographs of the scaffolds were chosen from Z-Stack images that were prepared using an FV1000 Viewer (Olympus, Tokyo, Japan) and collected every 5 μm to examine cell migration.

The procedure of staining for vimentin (60330-1-Ig; Wuhan Sanying, China), phosphoenolpyruvate carboxykinase (PCK; 16754-1-AP; Wuhan Sanying, China) and DAPI (C1002; Beyotime Biotechnology, China) is the same as described above. The tissue immunofluorescent staining procedure is essentially the same for the cells[24].

2.11. Ischemic buttons model (IBM)

The Jinling Hospital's Animal Investigation Ethics Committee authorized all of the animal care and experimental protocols, which were carried out in strict accordance with the Chinese Guidelines for the Care and Use of Laboratory Animals (Ministry of Science and Technology [2006] file no. 398). Pain was kept to a minimum by doing all procedures under anesthesia. Adhesion induction procedures were performed on wild-type B6 (C57BL/6J; GemPharmatech Co. Ltd., China) mice at 6–8 weeks. On the median line, a skin incision was made along the length of the abdomen. Based on the length of the peritoneum, a comparable midline abdominal incision was created in the peritoneum. The peritoneum was gently folded to the right and compressed with a hemostat. An ischemia button was inserted into the right side of the peritoneal wall after a tiny section of peritoneum (about 5 mm in diameter) was clamped with hemostatic forceps, the bottom of which was ligated with 4-0 silk (Suzhou Medical Co. Ltd., China), and the forceps were then released. Optionally, a light scrubbing of

Table 1. Adhesion score

Grade	Grade description
1	Filmy and easy to separate or separates spontaneously by accessing the peritoneal cavity.
2	Blunt dissection possible, beginning vascularization but no visible bleeding when separated.
3	Lysis possible by sharp dissection only, clear vascularization, visible bleeding when separated.
4	Lysis possible by sharp dissection only, organs strongly attached with severe adhesions, damage of organs when separated.

the button (20 times) and the adjacent liver, cecum, small intestine, and large intestine (7 times) could be performed with a surgical brush (depending on the desired severity of adhesions). The peritoneum and skin were closed with 4-0 silk sutures[25].

2.12. Adhesion scoring

All mice were given 200 mg/kg of ketamine hydrochloride and 10 mg/kg of xylazine hydrochloride to make them unconscious on postoperative days 1 and 7, after which the abdominal cavity was cut open in the middle of each animal. Adhesions were scored based on their tensile strength and vascularization as previously described (Table 1)[26].

2.13. Histological study

To carry out the histological study of the adhesion sites, representative samples were selected. The button and adherent tissues were excised, fixed in 4% buffered formaldehyde solution, embedded in paraffin sections, and stained with HE and Masson stain[27].

2.14. Statistical analysis

Data are expressed as mean ± SEM. Data were analyzed using GraphPad Prism 9 software by Student's *t* test (unpaired and two-tailed). The values were considered significantly different at $P < 0.05$.

3. Results and discussion

3.1. Fabrication of PCL scaffolds based on MEW

To obtain PCL scaffolds with fibers in a diversity of crossing angles, a custom-built MEW printer was used to deposit PCL onto a substrate with the assistance of a high-voltage electric field (Scheme 1). The printing path was predesigned in which the fibers were crossed at 30°, 60°, or 90°, because the angles may affect adhesion of cells loaded in the scaffolds[28,29]. The primary mesothelial cells were seeded on the PCL scaffolds to produce the peritoneal scaffolds, which aimed to form a barrier to separate the injured visceral organs from the abdominal wall physically and biologically.

We observed the morphology of MEW-printed PCL scaffolds. The PCL scaffolds were fabricated with a high resolution and satisfactory fidelity (Figure 1A–C). The fibers were 15–30 μm and arranged at the as-expected angles (30°, 60°, or 90°).

The PCL scaffolds presented different tensile stress–strain curves when the fibers were crossed differently (Figure 1D). The smaller crossing angles led to a significant reduction in tensile strength, Young's modulus, and fracture energy, and an increase in elongation length ratio at break (Figure 1E–H). This implied that the reduction of crossing angles lessened the stiffness, but increased the flexibility of the PCL scaffolds, which ensured that the scaffold adapted to the shear forces of organ movements.

The PCL scaffolds showed a hydrophobic property that interrupted the exchange of inflammatory exudate in the lesion site; therefore, they worked as a physical barrier for the prevention of tissue adhesion[30]. Reduction of the crossing angles of the fibers improved the hydrophobic property by presenting larger contact angles (Figure 1I).

3.2. Fabrication and optimization of peritoneal scaffolds

To mimic the composition and function of the peritoneum, we extracted murine primary peritoneal mesothelial cells as a constituent of the peritoneal scaffold (**Figure S1**). More than 90% cells were coexpressed with vimentin (red fluorescence) and PCK (green fluorescence), which indicated that the purity of primary peritoneal mesothelial cells was >90%. The mesothelial cells (Figure 2Ai) were seeded on the PCL scaffolds with different fiber angles (30°, 60°, and 90°) to screen the most suitable fiber arrangement for mesothelial cell growth (Figure 2Aii–iv). Light microscopy and immunofluorescence showed that mesothelial cells adhered to the PCL scaffolds (Figure 2B and C). Compared with the 60° and the 90° scaffolds, the 30° scaffold had a higher rate of mesothelial cell attachment (Figure 2D) and was more conducive to cell proliferation (Figure 2E).

Laronda *et al.*[29] have found that cell localization and survival in 3D-printed microporous hydrogel scaffolds depend on the geometry of the scaffold pores. The 30° and 60° scaffolds provided multiple edges to support cells, while the pores of 90° scaffolds limited cell–scaffold interactions. Cell survival was positively correlated with the number of strut contacts, which was improved as the amount of cell–scaffold interaction increased. Such a phenomenon also existed in the MEW-printed PCL scaffolds.

The scaffold fiber arrangement could guide the direction of cell proliferation. Mesothelial cells grew along the longitudinal axis on the 30° scaffolds (Figure 2Cii), but

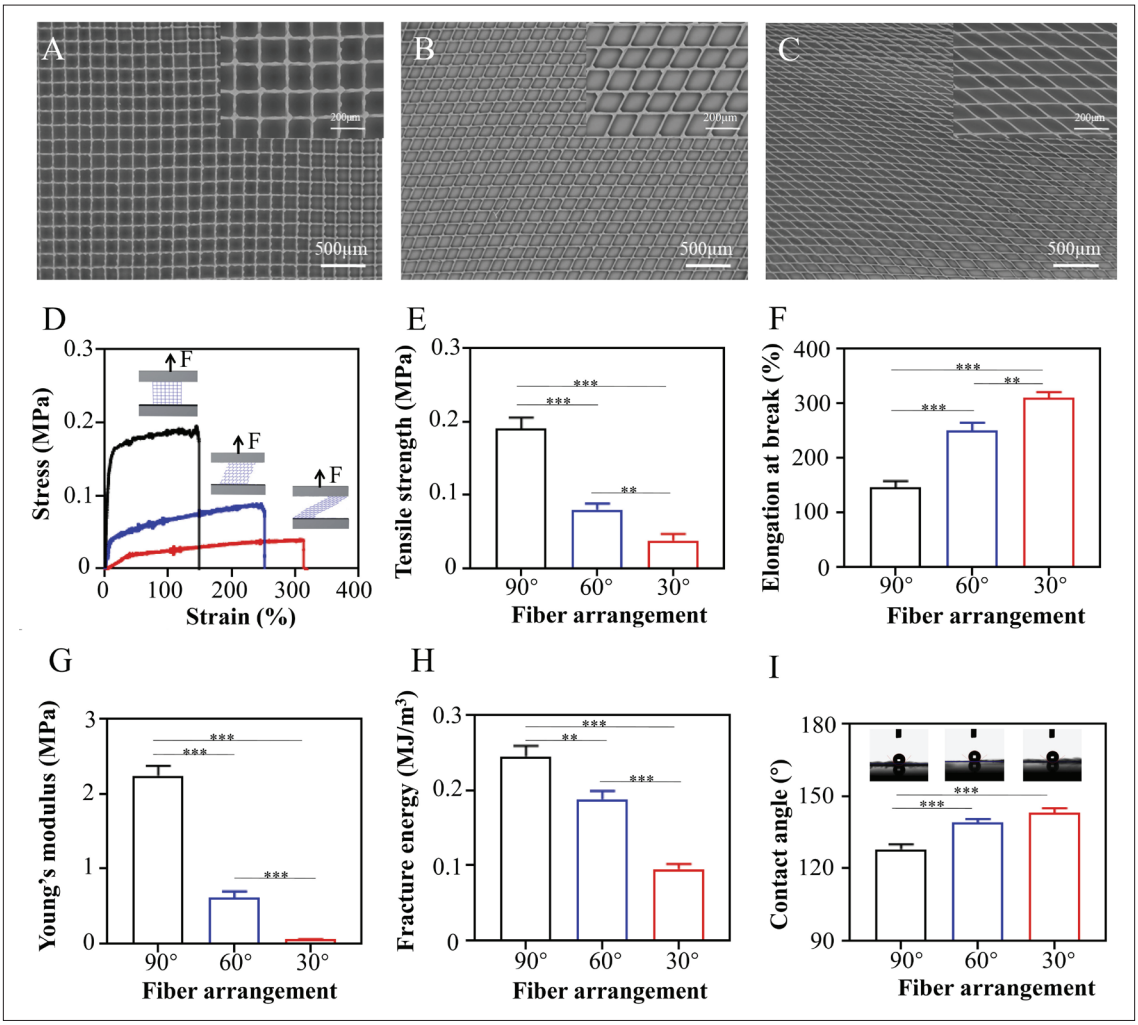

Figure 1. Structural and mechanical properties of PCL scaffolds with the fibers crossed at different angles. (A–C) The morphology of PCL scaffolds with the fibers crossed at 90° (A), 60° (B), and 30° (C). (D) Tensile strength–strain curve of PCL scaffolds with different fiber angles. (E) Tensile strength, n = 3. (F) Elongation at break, n = 3. (G) Young's modulus, n = 3. (H) Fracture energy, n = 3. (I) Contact angle, n = 3. $^{**}P < 0.01$; $^{***}P < 0.001$.

scattered centrifugally on the 60° scaffolds (Figure 2Ciii) and randomly on the 90° scaffolds (Figure 2Civ). This revealed that it was feasible to mimic the native arrangement of peritoneal mesothelial cells by inducing cells to grow orientationally rather than randomly or centrifugally with the 30° scaffold, which is important for tissue engineering[31]. The 30° scaffold was more conducive to the proliferation of mesothelial cells. Therefore, we chose the 30° scaffold to continue the study.

3.3. Barrier effects of the peritoneal scaffold *in vitro*

Previous studies have shown that abdominal macrophages play an important role in the formation of peritoneal adhesions[26]. Macrophages in the abdominal cavity can rapidly move to the site of injury and generate aggregates. The tissue connections bridging the aggregates and adjacent organs are thought to be the cornerstone of peritoneal adhesion formation. To investigate the potential mechanism of peritoneal scaffolds in the prevention of peritoneal adhesion, we constructed a cell Transwell model (Figure 3A, and **Figure S2**), which could measure the ability of scaffolds to hinder the recruitment and migration of adhesion-associated macrophages. The results indicated that migration of peritoneal resident macrophages was significantly reduced in the peritoneal scaffold group when compared with that in the simple PCL scaffold and blank groups (Figure 3B and C). This suggested the advantages of the peritoneal scaffold acting as a physical and biological barrier to block adhesion of the peritoneal injury site with other abdominal organs.

The selection of cell types is important when constructing a cell barrier for the prevention of peritoneal adhesions. For example, Tomoya *et al.*[24] proposed the

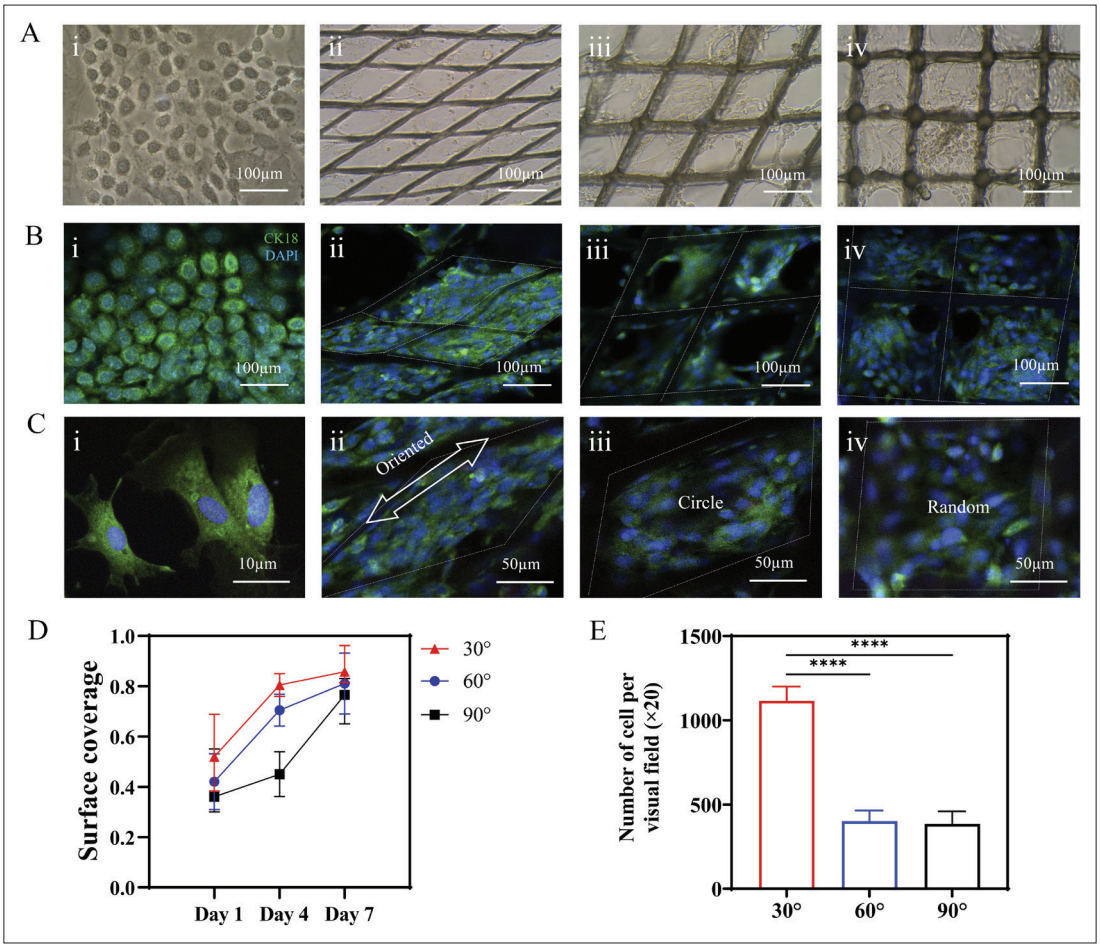

Figure 2. Behavior of peritoneal mesothelial cells growing on scaffolds with different pore shapes. (A) Representative images of cell morphology when cultured in (i) cell plate, or loaded by the scaffolds with the fiber angles at (ii) 30°, (iii) 60°, and (iv) 90°. (B) CK18 immunostaining of peritoneal mesothelial cells cultured on the cell plate or the scaffolds on day 7. (C) Magnified images of CK18 immunostaining on day 7. (D) Ratio of pores to loaded cells in the use of different scaffolds on days 1, 4, and 7. Magnification: 20×, n = 3. (E) Number of cells per visual field on the scaffolds with different pore shapes on day 7. Magnification: 20×, n = 3. ****$P < 0.0001$.

prevention of peritoneal adhesions by interleukin-4c-induced formation of a cellular barrier composed of peritoneal resident macrophages at the site of peritoneal injury. However, recent studies have shown that peritoneal resident macrophages are likely to be the driving factor in the formation of peritoneal adhesions[26]. This implies that the cell barrier is useful in the inhibition of adhesion, but the cell types and functions need further consideration. We chose peritoneal mesothelial cells to construct the peritoneal scaffold because they are the main component of the peritoneum and serve as a natural physiological barrier to lubricate the abdominal organs[15].

3.4. Degradation of the scaffold *in vivo*

Biodegradation of implanted biomaterials is a vital property because it can avoid iatrogenic injury of a second operation to remove the materials; therefore, we evaluated the degradation properties of the peritoneal scaffold *in vivo* (Figure 4). After 1 week of implantation, the mesh structure could be clearly seen in the peritoneal tissues (Figure 4A), which ensured that the peritoneal scaffold functioned as a qualified barrier during the acute phase of adhesion formation. The structure began to disintegrate and became fragmented in the second week (Figure 4B–E). Until the 16th week, the residual fragments of the scaffold were almost invisible (Figure 4F). The above experiments confirmed that the scaffold could be completely degraded *in vivo* for about 16 weeks and a second operation to remove the implanted scaffolds was unnecessary.

3.5. *In vivo* preventive effect of peritoneal scaffolds on peritoneal adhesions

To verify the use of peritoneal scaffolds for prevention of peritoneal adhesion *in vivo*, we implanted the scaffold into mice with IBMs (**Figure S3A** and **B**). On days 1 and 7 postoperatively, we evaluated the antiadhesive ability

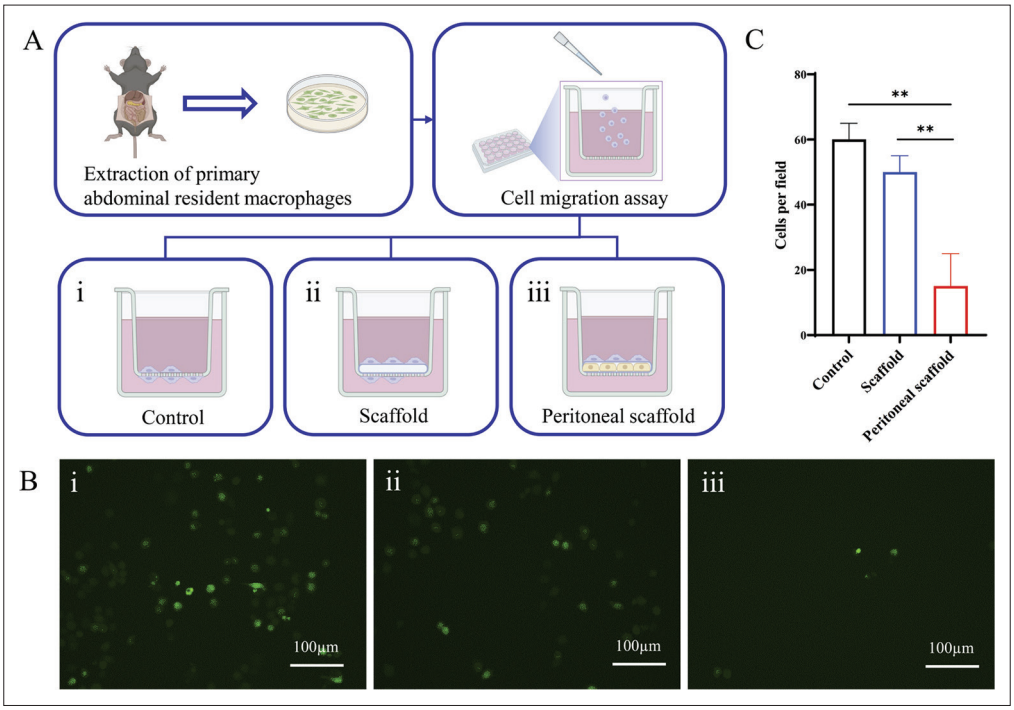

Figure 3. Effects of peritoneal scaffold on blocking macrophage migration verified with a Transwell assay. (A) Transwell cell models for measurement of scaffold's ability to inhibit migration of macrophages. Upper chambers: 100 μL serum-free DMEM and macrophages; lower chambers: 500 μL 20% DMEM as a chemoattractant. (i) Control group without placing PCL scaffold; (ii) placing simple PCL scaffolds; (iii) placing peritoneal scaffolds. (B) Immunofluorescence staining of migrated macrophages in the lower chamber after 12 h of coculture. (C) Quantitative analysis of migrated peritoneal macrophages, n = 3. $^{**}P < 0.01$.

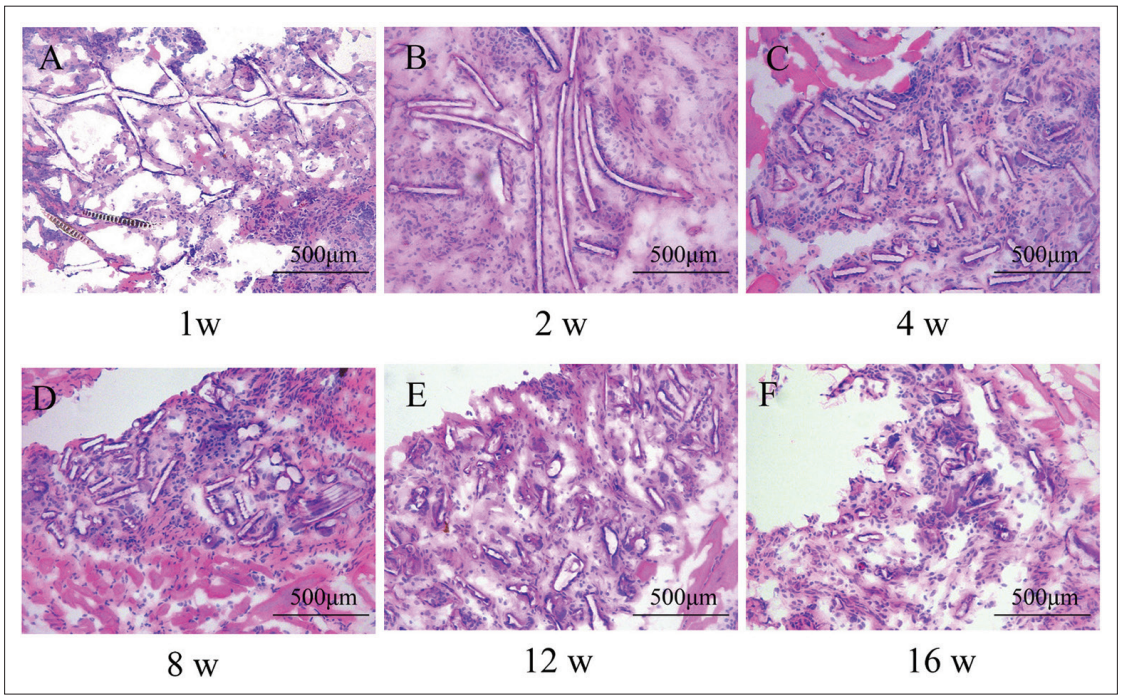

Figure 4. Evaluation of *in vivo* degradation after scaffold implantation. (A–F) HE staining confirmed the material biodegradability in mice at 1 (A), 2 (B), 4 (C), 8 (D), 12 (E), and 16 (F) weeks, postoperatively.

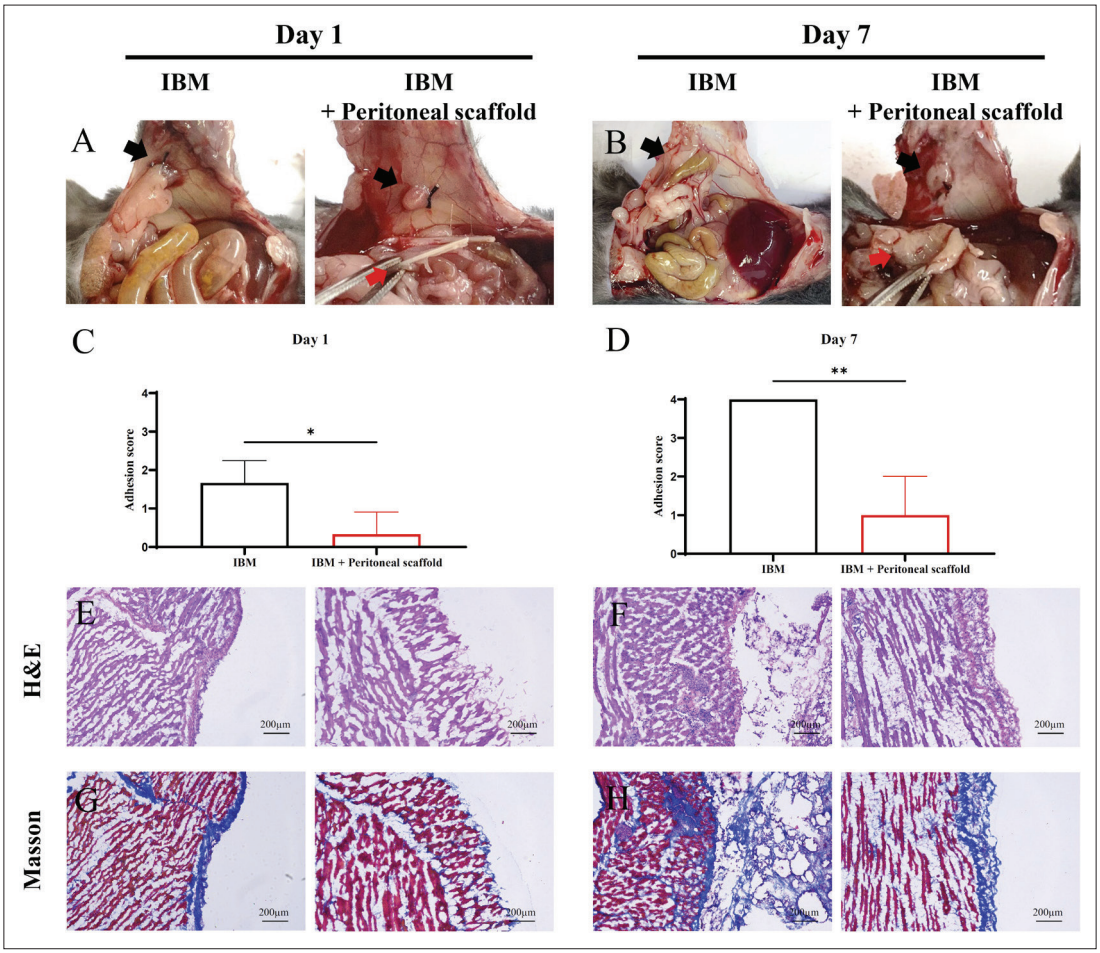

Figure 5. *In vivo* experiments of peritoneal scaffolds to prevent peritoneal adhesion. (A and B) Representative photographs of peritoneal adhesions in the blank control group and peritoneal scaffold group on days 1 and 7 postoperatively. Black arrow: adhesion area; red arrow: peritoneal scaffolds. (C and D) Adhesion score evaluation, n = 3. *$P < 0.05$; **$P < 0.01$. (E–H) Histological analysis of the lesion sites by HE and Masson staining in the IBM group and peritoneal scaffold group on days 1 and 7 postoperatively.

of peritoneal scaffolds *in vivo* using the adhesion score and histological staining methods (Figure 5A and B). In details, as for the control group, filamentous adhesion appeared on day 1, and it was further aggravated on day 7. Such adhesion could cause the injury of organs and peritoneum if surgical separation was performed. This showed the successful establishment of IBMs in mice. The peritoneal scaffold group had no adhesion on day 1. Blunt dissectable adhesion was formed on day 7, which was easily separated without bleeding. Intestinal flatulence was observed in the control group, suggesting the possible complication of intestinal obstruction, but this did not occur in the peritoneal scaffold group. Implantation of peritoneal scaffolds significantly decreased the peritoneal adhesion score in mice compared with the control group (Figure 5C and D).

Histological analysis showed that there was no obvious inflammatory cell infiltration in the peritoneal scaffold group on days 1 and 7 (Figure 5E and F). Peritoneal scaffolds did not lead to significant adverse effects on the healing of injured peritoneum. Masson staining showed that the peritoneal lesion of IBMs in the control group started to show fibrosis on day 1, and gradually formed a dense fibrous tissue layer on day 7. The thickness of the fibrous tissue layer in the peritoneal scaffold group was significantly lower than that in the control group on days 1 and 7 (Figure 5G and H). We demonstrated that the simple PCL scaffolds without carrying mesothelial cells were also susceptible to peritoneal adhesion (**Figure S4**), revealing the indispensable functions of the biological barrier generated by mesothelial cells.

Fetal liver mesothelial cell sheets fabricated by Inagaki *et al.* successfully prevented adhesion formation after hepatectomy[11]. Compared to our scaffold, the fetal liver mesothelial cell sheet was mechanically weak and difficult to be fixed, so it is difficult to adapt to intestinal peristalsis.

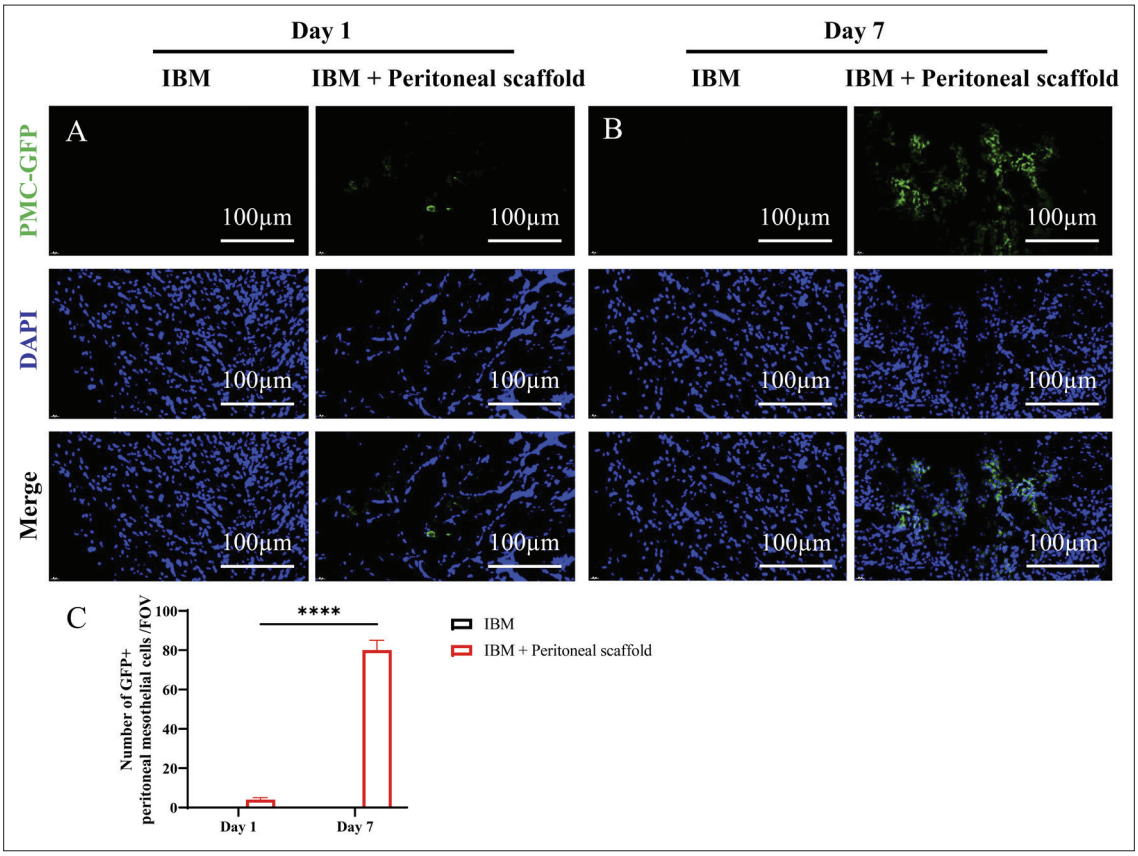

Figure 6. Peritoneal scaffolds directly participated in the repair of peritoneal damages revealed by *in vivo* tracking of GFP-labeled mesothelial cells. (A and B) Representative immunofluorescence staining of different groups on day 1 (A) and day 7 (B), postoperatively. (C) Quantification of the number of GFP$^+$ peritoneal mesothelial cells per field of view (FOV) in IBM group or IBM + peritoneal scaffold group. n = 3/group. ****$P < 0.0001$.

The peritoneal scaffold was based on the biodegradable and biocompatible PCL materials, with the advantage of good mechanical strength and easy fixation. The peritoneal scaffold was fabricated based on the MEW technology, which could be personalized according to different applications. The *in vivo* experiments confirmed that the peritoneal scaffold had good biosafety, and prevented the formation of intraperitoneal adhesion and inhibited fibrous tissue proliferation.

3.6. Promotion of peritoneal repair by the peritoneal scaffolds *in vivo*

To confirm whether the peritoneal scaffold could participate in the repair of the damaged peritoneum as expected, mesothelial cell tracking by *GFP* gene-contained lentivirus (**Figure S5**) was carried out. We were able to assess the mesothelial cell survival after implantation *in vivo*, and evaluate how the cells affected the repair of damaged peritoneal tissues. To our expectation, expression of GFP was seen at the injured peritoneal site on the first day after peritoneal scaffold implantation (Figure 6A). On day 7, the injured peritoneal site had higher GFP expression (Figure 6B and C). This suggests that the implanted peritoneal scaffold was directly involved in the repair of the damaged peritoneum.

4. Conclusions

Here, we reported an MEW-based peritoneal scaffold application for the first time to prevent peritoneal adhesion and promote the repair of injured peritoneum. The MEW-printed scaffold with the fibers crossed at 30° was screened due to the improved flexibility and hydrophobic property. Such a fiber angle also facilitated carriage of more mesothelial cells that grew in an orderly manner on the scaffold. The resultant peritoneal scaffolds inhibited migration of macrophages *in vitro* and prevented peritoneal adhesions *in vivo*. The use of primary peritoneal mesothelial cells was a highlight in the fabrication of cell-laden scaffolds because these cells were found to engage directly in the repair of injured peritoneum. The peritoneal scaffold is a novel attempt to solve the problem of peritoneal adhesions, and sets a good example of *in situ* repair based on cell-laden scaffolds for tissue engineering.

Acknowledgments

None.

Funding

This study was supported by the National Natural Science Foundation of China (82270595), Key Research and Development Program of Jiangsu Province (BE2022823), Postdoctoral Innovation Talents Support Program (BX20220393), and Postgraduate Research & Practice Innovation Program of Jiangsu Province (SJCX22_0031).

Conflict of interest

The authors declare no conflicts of interest.

Author contributions

Conceptualization: Xiuwen Wu, Huajian Ren
Formal analysis: Canwen Chen, Ze Li
Investigation: Jianan Ren, Huajian Ren
Methodology: Ziyan Xu, Kang Chen, Sicheng Li
Writing – original draft: Sicheng Li, Ye Liu
Writing – review & editing: Jinjian Huang, Sicheng Li

Ethics approval and consent to participate

The animal study was approved by the local animal ethics committee (approval number: 2022DZGKJDWLS-0069).

Consent for publication

Not applicable.

Availability of data

All data used in this work are presented in the paper and/or the Supplementary File.

References

1. Molegraaf MJ, Torensma B, Lange CP, *et al.*, 2017, Twelve-year outcomes of laparoscopic adhesiolysis in patients with chronic abdominal pain: A randomized clinical trial. *Surgery*, 161(2):415–421.

   https://doi.org/10.1016/j.surg.2016.08.014

2. Herrick SE, Allen JE, 2021, Surgical adhesions: A sticky macrophage problem. *Science*, 371(6533):993–994.

   https://doi.org/10.1126/science.abg5416

3. Ten BR, Issa Y, van Santbrink EJ, *et al.*, 2013, Burden of adhesions in abdominal and pelvic surgery: Systematic review and met-analysis. *BMJ*, 347(oct03 1):f5588.

   https://doi.org/10.1136/bmj.f5588

4. Krielen P, Stommel MWJ, Pargmae P, *et al.*, 2020, Adhesion-related readmissions after open and laparoscopic surgery: A retrospective cohort study (SCAR update). *Lancet (British edition)*, 395(10217):33–41.

   https://doi.org/10.1016/S0140-6736(19)32636-4

5. Wiseman DM, 2008, Disorders of adhesions or adhesion-related disorder: Monolithic entities or part of something bigger--CAPPS? *Semin Reprod Med*, 26(4):356–368.

   https://doi.org/10.1055/s-0028-1082394

6. Tang J, Xiang Z, Bernards MT, *et al.*, 2020, Peritoneal adhesions: Occurrence, prevention and experimental models. *Acta Biomater*, 116:84–104.

   https://doi.org/10.1016/j.actbio.2020.08.036

7. Trochsler M, Maddern GJ, 2014, Adhesion barriers for abdominal surgery: A sticky problem. *Lancet*, 383(9911):8–10.

   https://doi.org/10.1016/S0140-6736(13)62002-4

8. Ten BR, Stommel M, Strik C, *et al.*, 2014, Benefits and harms of adhesion barriers for abdominal surgery: A systematic review and meta-analysis. *Lancet*, 383(9911):48–59.

   https://doi.org/10.1016/S0140-6736(13)61687-6

9. Carmichael SP, Shin J, Vaughan JW, *et al.*, 2022, Regenerative medicine therapies for prevention of abdominal adhesions: A scoping review. *J Surg Res*, 275:252–264.

   https://doi.org/10.1016/j.jss.2022.02.005

10. Ito T, Shintani Y, Fields L, *et al.*, 2021, Cell barrier function of resident peritoneal macrophages in post-operative adhesions. *Nat Commun*, 12(1):2232.

    https://doi.org/10.1038/s41467-021-22536-y.

11. Inagaki NF, Inagaki FF, Kokudo N, *et al.*, 2015, Use of mouse liver mesothelial cells to prevent postoperative adhesion and promote liver regeneration after hepatectomy. *J Hepatol*, 62(5):1141–1147.

    https://doi.org/10.1016/j.jhep.2014.12.010

12. van Baal JO, Van de Vijver KK, Nieuwland R, *et al.*, 2017, The histophysiology and pathophysiology of the peritoneum. *Tissue Cell*, 49(1):95–105.

    https://doi.org/10.1016/j.tice.2016.11.004

13. Mutsaers SE, Prele CM, Pengelly S, *et al.*, 2016, Mesothelial cells and peritoneal homeostasis. *Fertil Steril*, 106(5):1018–1024.

    https://doi.org/10.1016/j.fertnstert.2016.09.005

14. Capobianco A, Cottone L, Monno A, *et al.*, 2017, The peritoneum: Healing, immunity, and diseases. *J Pathol*, 243(2):137–147.

    https://doi.org/10.1002/path.4942

15. Mutsaers SE, Prêle CM, Pengelly S, *et al.*, 2016, Mesothelial cells and peritoneal homeostasis. *Fertil Steril*, 106(5):1018–1024.

https://doi.org/10.1016/j.fertnstert.2016.09.005

16. Koffler J, Zhu W, Qu X, *et al.*, 2019, Biomimetic 3D-printed scaffolds for spinal cord injury repair. *Nat Med*, 25(2):263–269.

https://doi.org/10.1038/s41591-018-0296-z

17. Kim BS, Kwon YW, Kong JS, *et al.*, 2018, 3D cell printing of in vitro stabilized skin model and in vivo pre-vascularized skin patch using tissue-specific extracellular matrix bioink: A step towards advanced skin tissue engineering. *Biomaterials*, 168:38–53.

https://doi.org/10.1016/j.biomaterials.2018.03.040

18. Murphy SV, De Coppi P, Atala A, 2020, Opportunities and challenges of translational 3D bioprinting. *Nat Biomed Eng*, 4(4):370–380.

https://doi.org/10.1038/s41551-019-0471-7

19. Mandrycky C, Wang Z, Kim K, *et al.*, 2016, 3D bioprinting for engineering complex tissues. *Biotechnol Adv*, 34(4):422–434.

https://doi.org/10.1016/j.biotechadv.2015.12.011

20. Ye W, Xie C, Liu Y, *et al.*, 2021, 3D printed high-resolution scaffold with hydrogel microfibers for providing excellent biocompatibility. *J Biomater Appl*, 35(6):633–642.

https://doi.org/10.1177/0885328220962606

21. Tylek T, Blum C, Hrynevich A, *et al.*, 2020, Precisely defined fiber scaffolds with 40 μm porosity induce elongation driven M2-like polarization of human macrophages. *Biofabrication*, 12(2):25007.

https://doi.org/10.1088/1758-5090/ab5f4e

22. Huang J, Liu Y, Chi X, *et al.*, 2021, Programming electronic skin with diverse skin-like properties. *J Mater Chem A*, 9(2):963–973.

https://doi.org/10.1039/D0TA09101D

23. Huang J, Jiang Y, Liu Y, *et al.*, 2021, Marine-inspired molecular mimicry generates a drug-free, but immunogenic hydrogel adhesive protecting surgical anastomosis. *Bioact Mater*, 6(3):770–782.

https://doi.org/10.1016/j.bioactmat.2020.09.010

24. Ito T, Shintani Y, Fields L, *et al.*, 2021, Cell barrier function of resident peritoneal macrophages in post-operative adhesions. *Nat Commun*, 12(1):2232.

https://doi.org/10.1038/s41467-021-22536-y

25. Tsai JM, Sinha R, Seita J, *et al.*, 2018, Surgical adhesions in mice are derived from mesothelial cells and can be targeted by antibodies against mesothelial markers. *Sci Transl Med*, 10(469):n6735.

https://doi.org/10.1126/scitranslmed.aan6735

26. Zindel J, Peiseler M, Hossain M, *et al.*, 2021, Primordial GATA6 macrophages function as extravascular platelets in sterile injury. *Science*, 371(6533):e595.

https://doi.org/10.1126/science.abe0595

27. Zhang W, Wang X, Ma J, *et al.*, 2022, Adaptive injectable carboxymethyl cellulose/poly (gamma-glutamic acid) hydrogels promote wound healing. *Biomater Adv*, 136:212753.

https://doi.org/10.1016/j.bioadv.2022.212753

28. Xie C, Gao Q, Wang P, *et al.*, 2019, Structure-induced cell growth by 3D printing of heterogeneous scaffolds with ultrafine fibers. *Mater Design*, 181:108092.

https://doi.org/10.1016/j.matdes.2019.108092

29. Laronda MM, Rutz AL, Xiao S, *et al.*, 2017, A bioprosthetic ovary created using 3D printed microporous scaffolds restores ovarian function in sterilized mice. *Nat Commun*, 8(1):15261.

https://doi.org/10.1038/ncomms15261

30. Liang W, He W, Huang R, *et al.*, 2022, Peritoneum-inspired Janus porous hydrogel with anti-deformation, anti-adhesion, and pro-healing characteristics for abdominal wall defect treatment. *Adv Mater*, 34(15):2108992.

https://doi.org/10.1002/adma.202108992

31. Li Y, Lv S, Yuan H, *et al.*, 2021, Peripheral nerve regeneration with 3D printed bionic scaffolds loading neural crest stem cell derived Schwann cell progenitors. *Adv Funct Mater*, 31(16):2010215.

https://doi.org/https://doi.org/10.1002/adfm.202010215